Cytotoxic *trans*-Oriented Platinum Complexes only Form Adducts with Single-Stranded Oligodeoxynucleotides

Jo Vinje,[a] Francesco P. Intini,[b] Giovanni Natile,[b] and Einar Sletten*[a]

Abstract: The reactions of the anticancer complex *trans*-[$PtCl_2$\{(*E*)-HN=C(OMe)Me\}$_2$] (*trans-EE*) with both single-stranded and double-stranded deoxyribonucleotides have been studied by HPLC and 2D [^{1}H,^{15}N] HMQC NMR spectroscopy and compared with those of *cis*-[$PtCl_2(NH_3)_2$] (*cis*-DDP). Reactions of *trans-EE* with the single-stranded oligonucleotides d(CCTCGCTCTC) and d(CCTGGTCC) proceed rapidly through solvolysis of the starting substrate and subsequent formation of G-N7/monochloro *trans-EE* adducts. The rate of reaction is comparable to that of formation of an adduct from *trans-EE* and the dinuclotide d(ApG). Quite unexpectedly, the double-helical duplexes, d(TATGGTACCATA)$_2$ and d(TATGGCCATA)$_2$, with no terminal G residues, are practically inert towards *trans-EE*, and only minor species (<5% as estimated from HPLC traces) appear during 24 h reaction time. However, the duplexes d[(CCTCGCTCTC)·(GAGAGCGAGG)] and d(GATAGGCCTATC)$_2$, which contain both terminal and central G residues, undergo platination only at the terminal, solvent-exposed, G residues, thereby confirming that the interior of the duplex is not accessible to *trans-EE* due to steric hindrance. In contrast, *cis*-DDP was found to bind exclusively to the central GG pair in d(GATAGGCCTATC)$_2$.

Keywords: antitumor agents · DNA · kinetics · oligonucleotides · platinum complexes

Introduction

The well-known anticancer drug *cis*-diamminedichloroplatinum(II) (*cis*-DDP) can form a variety of covalent DNA adducts. Although the structure–activity relationship underpinning the high efficacy of *cis*-DDP in the treatment of cancers is not fully understood, it is generally believed that the cytotoxic properties are a consequence of its bifunctional binding to DNA.[1] In the major adduct, *cis*-DDP forms 1,2-cross-links between adjacent purines in d(GpG) or d(ApG) sequences.[2] These lesions result in a bending of the helical axis of DNA by 25–50° in the direction of the major groove.[3–6] The clinically ineffective *trans*-DDP isomer cannot form these types of 1,2-N7,N7 adducts.

Recently it has been shown that several analogues of *trans*-DDP exhibit antitumor properties.[6] Early examples of active *trans*-Pt^{II} complexes were the *trans*-[$PtCl_2$(pyridine)$_2$] and the *trans*-[$PtCl_2$(imino ether)$_2$] species.[7–9]

Farell and co-workers found that *trans*-platinum complexes with planar ligands may be as cytotoxic as *cis*-DDP and dramatically more cytotoxic than *trans*-DDP.[10] In cellular systems this type of compound, for example, *trans*-[$PtCl_2$(pyridine)$_2$], was found to accumulate more rapidly than the DDP complexes. However, in cell-free systems, *trans*-[$PtCl_2$(pyridine)$_2$] was shown to bind to DNA significantly less (approximately 5–10-fold) than *cis*- or *trans*-DDP.[10]

Of particular interest were the compounds with imino ether ligands, such as *trans*-[$PtCl_2$\{(*E*)-HN=C(OMe)Me\}$_2$] (*trans-EE*, see below), which have shown an activity comparable to that of *cis*-DDP in the P338 leukaemia system and exert antitumor effects on Lewis lung carcinoma.[7,11] Imino ether ligands share some features with both amines and pyr-

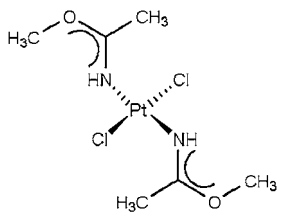

[a] J. Vinje, Prof. Dr. E. Sletten
Department of Chemistry
University of Bergen
Allègt. 41, 5007 Bergen (Norway)
Fax: (+47) 5558-9490
E-mail: einar.sletten@kj.uib.no

[b] Dr. F. P. Intini, Prof. Dr. G. Natile
Dipartimento Farmaco-Chimico
University of Bari
via E. Orabona 4, 70125 Bari (Italy)

Supporting information for this article is available on the WWW under http://www.chemeurj.org/ or from the author.

 DOI: 10.1002/chem.200400118

idine-like ligands. Like pyridine, imino ethers are planar (sp^2-hybridized nitrogen atom); however, like amines, they have one hydrogen atom that is linked to the nitrogen atom and is suitable for hydrogen-bond formation. Moreover, imino ether ligands are nonsymmetrical, with the steric hindrance concentrated on the side of the nitrogen atom opposite to that of the proton.

The *trans-EE*/DNA binding mode in cell-free media has been investigated by several biophysical methods. The major DNA lesion formed by *trans-EE* appears to be a monofunctional Pt binding to the N7 nitrogen atom of a purine base.[12] Recently we have published a structural analysis of a *trans-EE* platinated duplex formed by platination at G-N7 of the single-stranded 5′-d(CCTCG*CTCTC) sequence and subsequent hybridization with its complement 5′-d(GAGAGCGAGG) (G* indicates a platinated guanine).[13] Interestingly, *trans-EE* platination was found to induce a bending of the helix axis towards the minor groove by 45°. The magnitude of this bending angle is comparable to that observed in 1,2-bifunctional adducts of *cis*-DDP, although in the latter case the bending is directed towards the major groove. Subsequent gel-electrophoretic studies by Brabec and co-workers[14] showed that *trans-EE* induces DNA bending of approximately 21° towards the minor groove at the guanine residues.

The cellular accumulation of *trans-EE* is greatly enhanced (>50-fold) with respect to that of cisplatin.[6] A possible explanation for the marked accumulation of this compound can be found in the enhanced lipophilicity of the carrier ligands.

It is also to be noted that, apart from the disubstituted compounds described above, the replacement of only one ammine group in *trans*-DDP by a bulky, rather planar, ligand is sufficient for activation of the *trans* geometry.[6,8,15]

In most reported studies on the kinetics of monofunctional platination of single- and double-stranded oligonucleotides, NMR spectroscopic and chromatographic methods have been used to determine kinetic parameters. Recently, we have published a comprehensive study of the kinetics of monofunctional binding of $[Pt(dien)Cl]^+$ to a series of self-complementary deoxyribonucleotides,[16] with results showing that the affinity for the nitrogen atom of the G residue on the 5′-side follows the order: 5′-GG > GA > GT ≫ GC. In this paper we wish to address both the question of selectivity and the differences in kinetics between single- and double-stranded oligodeoxyribonucleotides for the binding of *trans-EE*.

Results

The following experiments were performed:

1) *trans-EE* versus single-stranded d(CCTCGCTCTC) (**V**) and d(CCTGGTCC) (**VI**). The reactions were carried out with an equimolar ratio of reactants, $T = 298$ K.
2) *trans-EE* versus duplexes $d(TATGGTACCATA)_2$ (**I**) and $d(TATGGCCATA)_2$ (**II**) with substoichiometric, equimolar, and excess platinum conditions, $T = 298$ and 310 K.
3) *trans-EE* versus duplex d[(CCTCGCTCTC)·(GAGAGCGAGG)] (**III**), first with an equimolar ratio and then with threefold excess of platinum, $T = 298$ K.
4) *trans-EE* versus duplex $d(GATAGGCCTATC)_2$ (**IV**) with 1:2 and 1:1 Pt/duplex ratios, $T = 285$ and 298 K.
5) Control experiments of *cis*-DDP versus **V** and **IV** with equimolar concentrations of reactants, $T = 298$ K.

The NMR proton signals of all double-stranded oligonucleotides except **IV** (**I**–**III**) were already assigned.[13,16] The proton resonances of **IV** were assigned by using the well-known method of sequential connectivity of 2D [^{1}H,^{1}H] NOESY cross-peaks for right-handed double-helical DNA. The magnitude of the cross-peaks in the 2D [^{1}H,^{1}H] NOESY maps for the duplex indicated normal B-form geometry. The spectra of the imino region exhibited all the expected Watson–Crick thymine and guanine imino signals up to 298 K; at higher temperatures the terminal guanine imino signal disappears. The signals for single-stranded **V** were assigned from long-mixing-time 2D [^{1}H,^{1}H] NOESY spectra. The 1D ^{1}H spectrum was well resolved, which indicates that **V** has an ordered conformation. From the 2D [^{1}H,^{1}H] NOESY spectra the cytosines were determined from the strong H6–H5 cross-peaks. The thymines were assigned from the methyl–H6 cross-peaks. The guanine H8 signal was found to be the most downfield-shifted signal. The signal assignments for **VI** were done in the same way. The numbering of the nucleobases in the oligonucleotides is from 5′ to 3′, for example, duplex **III** is 5′-d($C^1C^2T^3C^4G^5C^6T^7C^8T^9C^{10}$)·($G^{11}A^{12}G^{13}A^{14}G^{15}C^{16}G^{17}A^{18}G^{19}G^{20}$).

Reaction of d(CCTCGCTCTC) (V) with *trans-EE*: The reaction between *trans-EE* and **V** was carried out with a Pt/**V** ratio of 4:3 and at pH 3.5. The 1D ^{1}H NMR spectrum (region of nucleotide aromatic protons) showed a new downfield-shifted G^5-H8 signal at 0.37 ppm and also a downfield shift of the C^6-H6 signal by approximately 0.15 ppm into the group of peaks at 7.98–8.09 ppm (Figure 1a). In a previous NMR spectroscopy study of G^5-platinated duplex **III** (**V** is coincident with the pyrimidine-rich strand of **III** and it was G^5-platinated and subsequently annealed with its complementary strand) similar downfield shifts were observed for the G^5-H8 and C^6-H6 signals.[13]

The 2D [^{1}H,^{15}N] HMQC spectra (imino ether protons) initially show three peaks at 7.40/86.92, 7.57/86.39, and 7.69/89.27 ppm (Figure 2a). The first peak corresponds to dichloro *trans-EE*, the second to monoaqua monochloro *trans-EE*, and the third to G-N7/monochloro *trans-EE*. The assignment of dichloro *trans-EE* and monoaqua monochloro *trans-EE* in Figure 2 is based on 2D [^{1}H,^{15}N] HMQC spectra recorded for an aqueous solution of pure dichloro *trans-EE* at the same pH value and salt concentration as used in the experiment of Figure 2. The monoaqua monochloro *trans-EE* signal has a lower ^{15}N shift than that published earlier by Liu et al. ($\delta = 7.52/90.5$ ppm)[17] because of the lower pH value in the present experiment. The G-N7/monochloro *trans-EE* peak is assigned based on the simultaneous ap-

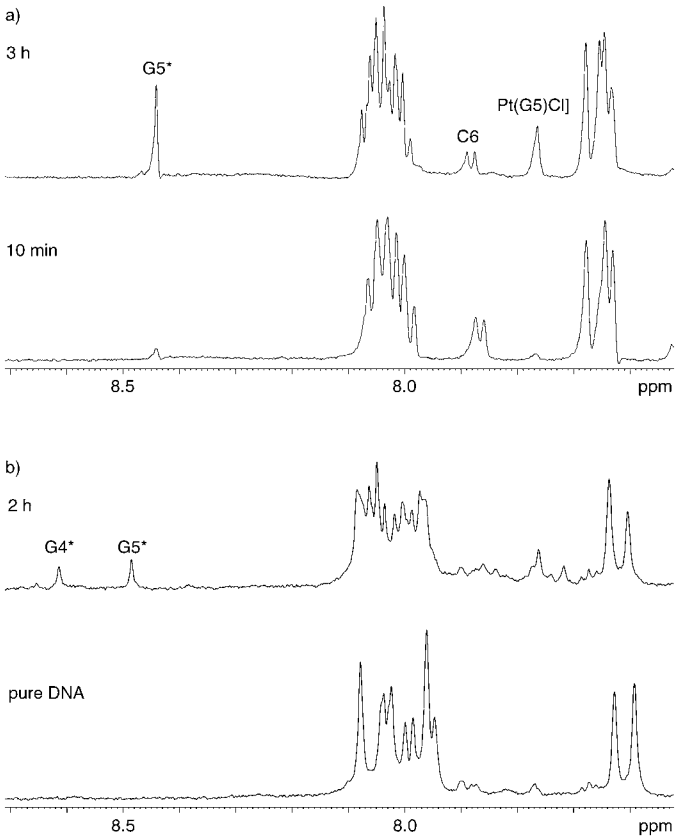

Figure 1. Aromatic region of 1D ^{1}H NMR spectra for the reaction of a) 1.2 mM *trans-EE* and 0.90 mM **V** (pH 3.5, 20 mM $NaClO_4$, 20 mM phosphate buffer) and b) 1.5 mM *trans-EE* and 1.5 mM **VI** (pH 3.0, 20 mM $NaClO_4$). The platinated G residues are marked with an asterisk (*).

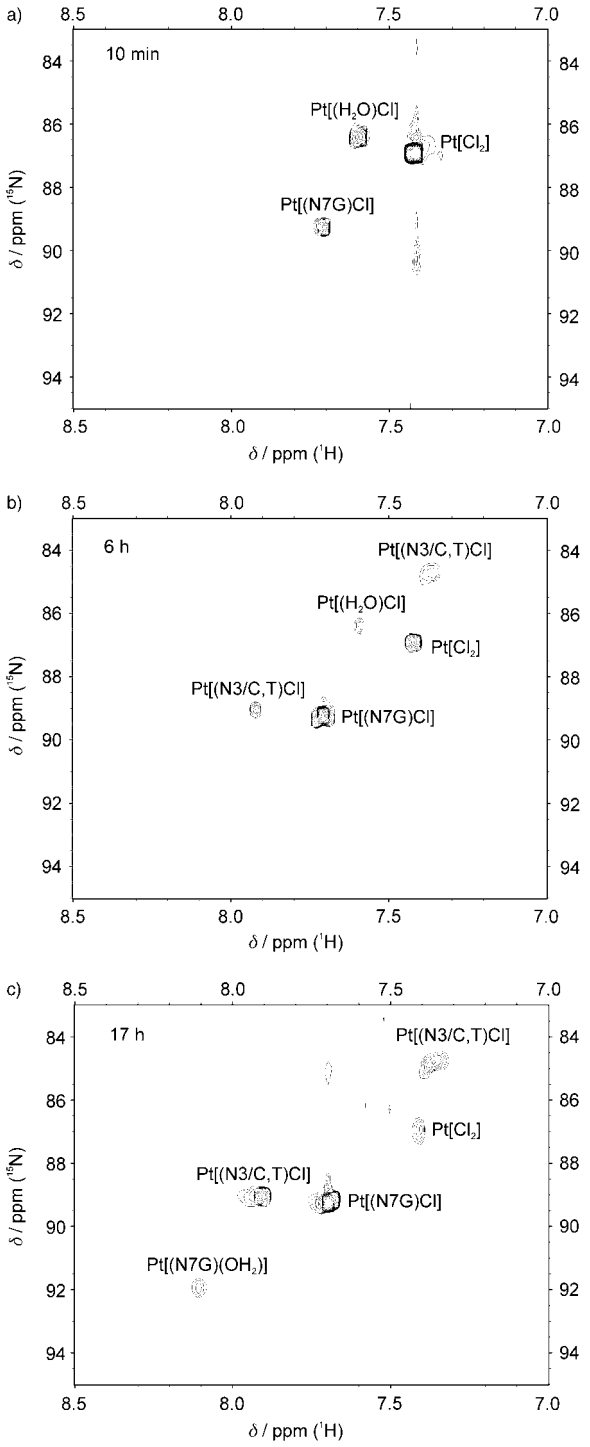

Figure 2. 2D [^{1}H,^{15}N] NMR spectra of 1.2 mM *trans-EE* and 0.90 mM **V** (pH 3.5, 20 mM $NaClO_4$, 20 mM phosphate buffer).

pearance in the 1D ^{1}H NMR spectra of a downfield-shifted G^5-H8 signal that is indicative of guanine platination.

After 1.5 h, two new signals appear at 7.34/84.71 and 7.90/89.03 ppm (Figure 2b). These signals may represent binding to cytosine or thymine residues since the absence of a new downfield-shifted G^5-H8 signal in the 1D ^{1}H NMR spectra indicates that no new *trans-EE*/G-N7 species have been formed. Therefore, the binding must involve cytosine or thymine for which platination at N3 induces only a minor shift of the signals of the aromatic protons H6 and H5.

After 9.5 h, a peak emerges at 8.10/91.87 ppm in the 2D [^{1}H,^{15}N] HMQC spectra (Figure 2c). At the same time the 1D ^{1}H NMR spectra show a new G^5-H8 peak 0.03 ppm downfield of the G-N7/monochloro *trans-EE* signal. The intensity of the new peak in the 1D ^{1}H NMR spectra is correlated with the intensity of the signal at 8.10/91.87 ppm in the HMQC spectra. In previous studies the G^5-H8 signal of G-N7/monoaqua *trans-EE* was found to appear slightly downfield of the peak of G-N7/monochloro *trans-EE*;[17,18] therefore, the peak at 8.10/91.87 ppm is assigned to G-N7/monoaqua *trans-EE*.

Experimental concentrations evaluated from NMR spectroscopic data and theoretically fitted curves for this reaction are reported in Figure 3a. Evaluated rate constants are reported in Table 1.

Reaction of d(CCTGGTCC) (VI) with *trans-EE*: Dichloro *trans-EE* and **VI** were reacted at equimolar amounts in 20 mM $NaClO_4$ (pH 3.0). The 1D ^{1}H spectra show two new G-H8 peaks shifted 0.53 ppm and 0.40 ppm downfield and representing G^4- and G^5-platinated residues, respectively. The two signals have similar intensities (Figure 1b). The 2D [^{1}H,^{15}N] HMQC spectra initially show three peaks at 7.40/87.59, 7.57/86.33 and 7.71/89.29 ppm; these correspond to dichloro *trans-EE*, monoaqua monochloro *trans-EE*, and G-

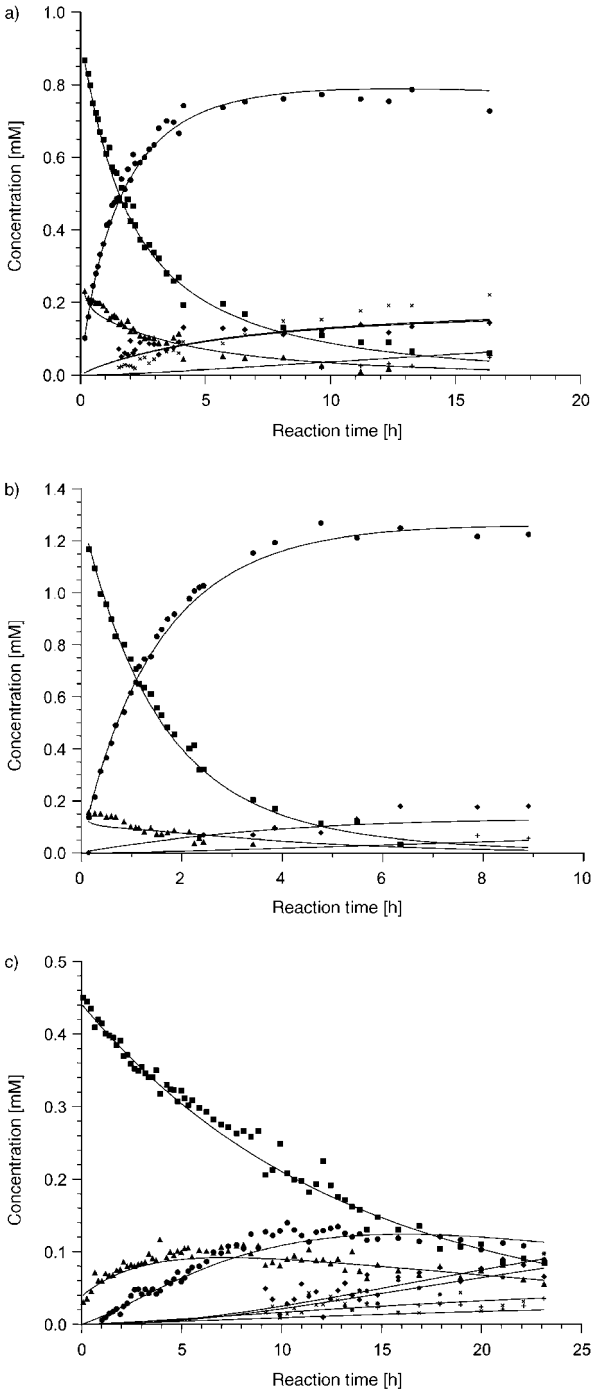

Figure 3. Experimental concentrations (NMR data) and theoretically fitted curves for the reactions between a) 1.2 mM *trans-EE* and 0.90 mM **V** (pH 3.5, 20 mM $NaClO_4$, 20 mM phosphate buffer), b) 1.5 mM *trans-EE* and 1.5 mM **VI** (pH 3.0, 20 mM $NaClO_4$), and c) 0.48 mM *cis*-DDP and 0.50 mM **V** (pH 6.0, 20 mM $NaClO_4$). All experiments were performed at 298 K. Symbols for a) and b): (■) dichloro *trans-EE*, (▲) monoaqua monochloro *trans-EE*, (●) G-N7/monochloro *trans-EE*, (◆) and (×) C-N3/monochloro *trans-EE* or T-N3/monochloro *trans-EE*, (+) G-N7/monoaqua *trans-EE*. Symbols for c): (■) dichloro *cis*-DDP, (▲) monoaqua monochloro *cis*-DDP, (●) G-N7/monochloro *cis*-DDP, (◆) and (*) *cis*-DDP/[(G-N7)(C-N3)], (+) and (×) C-N3/monochloro *cis*-DDP or T-N3/monochloro *cis*-DDP.

N7/monochloro *trans-EE* species, respectively. Evidently, the G^4 and G^5 adducts are represented by a single cross-peak. A fourth peak ($\delta = 7.94/89.18$ ppm), which appears after 2 h of reaction time, is tentatively assigned to C-N3/monochloro *trans-EE* or T-N3/monochloro *trans-EE*. After about 8 h, a fifth peak occurs at 8.16/92.16 ppm; this corresponds to G-N7/monoaqua *trans-EE* (as for **V**).

Experimental concentrations evaluated from NMR spectrosopic data and theoretically fitted curves for this reaction are reported in Figure 3b. Evaluated rate constants are reported in Table 1.

Table 1. Platination rate constants (standard deviation in parentheses) for the reaction of *trans-EE* with single-stranded **V** and **VI** and duplexes **III** and **IV**.[a]

	k_{Pt-G} [$M^{-1}s^{-1}$]	$k_{Pt-C/T} \times 10^{-5}$ [s^{-1}]
V[b]	0.79 (3)	4.2 (3), 4.2 (3)
VI[c]	1.47 (9)	8 (1)
III[d]	1.9 (4), 1.0 (2), 0.38 (9)	
IV[e]	1.0 (2)	
IV[f]	0.107 (3)	

[a] Kinetic equations and defining rate constants are given in the Supporting Information. [b] 298 K, 20 mM $NaClO_4$, 20 mM phosphate buffer, pH 3.5. [c] 298 K, 20 mM $NaClO_4$, pH 3.0. [d] 298 K, 20 mM $NaClO_4$, 20 mM phosphate buffer, pH 5.7. The three values represent binding to 5′-G^1, G^9, and G^{10} on the lower strand. [e] 298 K, 100 mM $NaClO_4$, pH 5.8. [f] 285 K, 100 mM $NaClO_4$, pH 6.0, kinetic fit shown in Figure S1.

Reaction of d(CCTCGCTCTC) (V) with *cis*-DDP: In a control experiment, *cis*-DDP was allowed to react with **V** at equimolar concentration. The reaction was performed at pH 6.0 to avoid the overlap observed when performing the same experiment at lower pH values. The 1D ^1H spectrum exhibits a G-H8 signal shifted 0.35 ppm downfield, a result characteristic of N7 platination. Initially, the 2D [^1H,^{15}N] HMQC spectra only show the peaks from dichloro *cis*-DDP (4.04/−69.14 ppm) and monoaqua monochloro *cis*-DDP (4.23/−67.38 and 4.07/−88.54 ppm). The peaks corresponding to G-N7/monochloro *cis*-DDP (4.09/−69.48 and 4.37/−66.08 ppm) appear after 1 h. After 9 h, two new peaks occur at 4.07/−67.44 and 4.40/−65.87 ppm. After 14 h, three other peaks occur at 4.20/−70.44, 4.30/−70.70, and 4.35/−71.79 ppm. The sample was checked again after one week to see which of these new peaks correspond to GC cross-links and which represent monofunctional cytosine or thymine adducts. The spectrum after 1 week showed five peaks at 4.26/−68.80, 4.30/−70.61, 4.35/−71.79, 4.38/−64.90, and 4.40/−65.91 ppm. Therefore, the peaks at 4.30/70.70, 4.35/−71.79, and 4.40/−65.87 (present in the spectra taken after 9 and/or 14 h and also in that taken after one week) represent cross-linked GC adducts while the peaks at 4.07/−67.44 and 4.20/−70.44 ppm (present in the spectra taken after 9 and/or 14 h but absent in that taken after one week) represent monofunctional cytosine or thymine adducts. The two peaks at 4.30/70.70 and 4.35/−71.79 ppm occurred at the same time and are of equal intensity and were therefore assigned to the same GC cross-linked adduct. The signal at 4.40/−65.87 ppm does not have a corresponding peak. (The fact that the peak at 4.07/−67.44 has disappeared after one week rules out the possibility that this peak corresponds to a peak of a cross-linked adduct.) Therefore, for this GC cross-linked adduct the second peak must be hidden underneath the water signal. Thus, the intensity of the peak at 4.40/

−65.87 ppm was multiplied by two in order to have the correct concentration of the second GC adduct.

Experimental concentrations evaluated from NMR spectroscopic data and theoretically fitted curves for this reaction are reported in Figure 3c. Evaluated rate constants are reported in Table 2.

Table 2. Platination rate constants (standard deviation in parentheses) for the reaction of dichloro *cis*-DDP with single-stranded **V** and duplex **IV** at 298 K.[a]

	k_{Pt-G} [$M^{-1}s^{-1}$]	$k_{chelate} \times 10^{-5}$ [s^{-1}]
V[b]	0.126 (4)	1.15 (5), 0.99 (6)
IV[c]	0.6 (1)	4.09 (7)

[a] Kinetic equations defining rate constants are given in the Supporting Information. [b] 20 mM $NaClO_4$, 20 mM phosphate buffer, pH 6.0. [c] 100 mM $NaClO_4$, pH 5.7.

Reaction of d(TATGGCCATA)$_2$ (I) with *trans-EE*: No apparent interaction was observed in a mixture of equimolar amounts of **I** and *trans-EE* (100 mM $NaClO_4$ and pH 6.8) monitored by NMR spectroscopy for 24 h at 298 K. The experiment was repeated at a lower pH value (4.1) and higher temperature (310 K) in order to increase the rate of opening of Watson–Crick base pairs and thus facilitate platination. In the 1D ^{1}H NMR spectrum the imino signals are absent, as expected, while the aromatic and methyl signals are still visible at similar shifts (to those seen when **I** was in a defined duplex conformation) but the peaks are broader. Therefore, it is possible to conclude that duplex **I** is not converted into single strands since, if this was the case, a completely new set of signals would appear at considerably different chemical shifts. Moreover, in single-stranded oligonucleotides the NMR signals are less separated, due to loss of stacking interactions and therefore loss of the ring-current chemical-shift effects seen in duplexes. Increasing the pH value to 6.6 restores the original spectrum of the unplatinated duplex, a result confirming that, even when the reaction is performed at lower pH value and higher temperature, the duplex is relatively inert and does not react with *trans-EE*.

In order to increase the reactivity of the platinum substrate, an analogous experiment was performed with the monochloro mononitrato *trans-EE* instead of the dichloro species. (The nitrato ligand undergoes fast solvolysis in water.) The reactants were mixed in a Pt/duplex ratio of 2:5 in 100 mM $NaClO_4$, at pH 5 and 298 K. As the reaction proceeds, several small new peaks appear in the NMR spectra and, after 24 h, the sum of these peaks is equivalent to 5–10% of the native duplex. In the 2D [^{1}H,^{15}N] HMQC spectra the initial monochloro monoaqua signal is slowly shifted to a new position. Further addition of platinum substrate (so as to bring the Pt/duplex ratio to slightly above 1:1) results in an increase of the reaction products, which then add up to 10–15% of the native duplex. After a total reaction time of 32 h, 1D ^{31}P NMR spectra were recorded in order to check if the platinum substrate was associated with the phosphate oxygen atoms of **I**. In a previous investigation it was shown that *trans-EE* can react with a phosphate buffer, thereby giving a ^{31}P signal that is shifted 6 ppm downfield;[19] however, in the present case no such a resonance was observed. The reaction products gave a set of cross-peaks in the 2D [^{1}H,^{1}H] NOESY map; however, the intensities were too low to allow a full sequential walk assignment.

Reaction of d(TATGGTACCATA)$_2$ (II) with *trans-EE*: Under different conditions from the previous case, this reaction was carried on in the presence of 20 mM phosphate buffer (1:1 Pt/duplex ratio, 100 mM $NaClO_4$, pH 2, and 310 K). The 2D [^{1}H,^{15}N] HMQC spectra were similar to those of **I** except for the presence of a monophosphato monochloro *trans-EE* adduct formed by interaction of the platinum substrate with the phosphate buffer. The 1D ^{1}H NMR spectra reveal the presence of a small amount of reaction products. The reaction mixture analyzed by HPLC exhibits one major peak and one broad minor peak (<5% of the major peak) that is assumed to be a platinated species (Figure 4a).

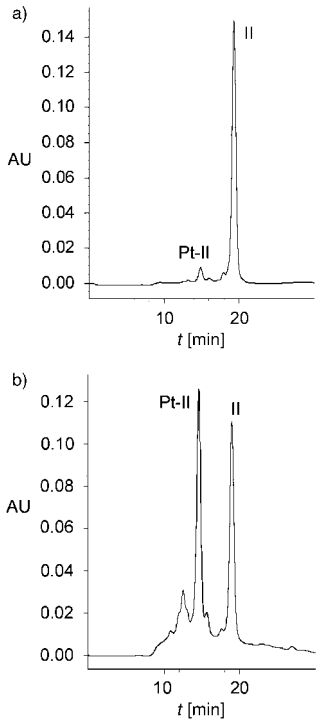

Figure 4. HPLC chromatograms of *trans-EE* and duplex **II** (100 mM $NaClO_4$, 20 mM phosphate buffer, pH 6.2) at: a) equimolar Pt/duplex ratio, 310 K, and 24 h reaction time and b) large excess of *trans-EE*, 330 K, and 5 h reaction time.

The reaction was repeated with a large excess of *trans-EE* and with heating of the sample to approximately 330 K for about 5 h. The HPLC trace showed two signals of similar intensities with retention times similar to those of the two peaks observed in the previous experiment (Figure 4b). The platinated fraction was analyzed by 1D ^{1}H and 2D [^{1}H,^{15}N] HMQC spectroscopy. The 1D ^{1}H NMR spectrum clearly showed that the platinated oligonucleotide was not in duplex form. An attempt was made to anneal the platinated single strands by heating above the melting temperature and

then slowly cooling the samples. This procedure did not yield a duplex, probably because the self-complementary sequence is hindered in forming a double-stranded adduct in which both the upper and lower strands would be platinated.

Reaction of d[(CCTCGCTCTC)·(GAGAGCGAGG)] (III) with *trans-EE*: The reaction was first performed by mixing equimolar amounts of duplex and *trans-EE* in 10 mM phosphate buffer and 15 mM $NaClO_4$ at pH 7 and 298 K. Initially, the 2D [^{1}H,^{15}N] HMQC spectra showed the presence of three peaks at 7.41/89.90, 7.55/89.00, and 7.67/89.72 ppm. The first two peaks correspond to dichloro *trans-EE* and monoaqua monochloro *trans-EE* species while the third peak corresponds to a *trans-EE*/**III** adduct. As the reaction proceeds the third peak increases, the dichloro *trans-EE* signal decreases, and a fourth peak becomes visible at 7.74/89.61 ppm; this probably corresponds to a second *trans-EE*/**III** adduct. After 4 h, 2 more peaks (5 and 6) appear at 7.99/91.33 and 8.38/92.26 ppm while the peaks of unreacted *trans-EE* (either dichloro or monoaqua monochloro) have disappeared. The two new peaks (5 and 6) probably correspond to the aquation products of the initially formed monofunctional platinum/G-N7 adducts (3 and 4). This conclusion is supported by the observation that peaks 3 and 4 decrease as peaks 5 and 6 increase; moreover, the chemical shifts of peaks 5 and 6 agree with the shifts observed for guanosine monophosphate (GMP)/monoaqua *trans-EE*.[17]

The 1D ^{1}H NMR spectra reveal that a signal downfield of the T^9 methyl signal has increased while the methyl signal of T^9 has decreased; also, the methyl signal of T^7 has decreased while two new signals, 0.033 and 0.022 ppm downfield of T7, have arisen. (The decrease in intensity of the T methyl signal accompanied by the increase in intensity of the new signal(s) downfield is less pronounced in T^7 than T^9.) In the aromatic region two new signals (8.183 and 8.126 ppm) increase while the H8 signals of A^{12} and A^{14} decrease and no change in intensity is observed for the A^{18}-H8 signal. In the imino region all the signals broaden and three new small signals become visible. The most likely interpretation of the above results is that one of the two products that formed initially is duplex **III** platinated at the terminal G^{11}. This explains the downfield-shifted T^9 methyl signal which is indicative of platination to a neighboring G base (either G^{11} or G^{13}). At the other end of the duplex, the signals from G^{19}-H8 and G^{20}-H8 decreased. This indicates platination at the two terminal G residues (G^{19} and G^{20}) as well. None of the interior G residues (G^5, G^{15}, and G^{17}) was found to be attacked by platinum. Experimental concentrations and theoretically fitted curves for the reaction between *trans-EE* and **III** (1:1.2 molar ratio) are reported in Figure 5a.

Reaction of d(GATAGGCCTATC)$_2$ (IV) with *trans-EE*: This duplex was designed with a "hot" central GG region and a terminal G residue. The reaction with *trans-EE* was carried out at 285 K, with a 2:5 Pt/duplex ratio and 100 mM $NaClO_4$ at pH 0. Initially the 2D [^{1}H,^{15}N] HMQC spectra show the presence of only one product (7.86/90.26 ppm) in addition to the dichloro and monoaqua monochloro *trans-*

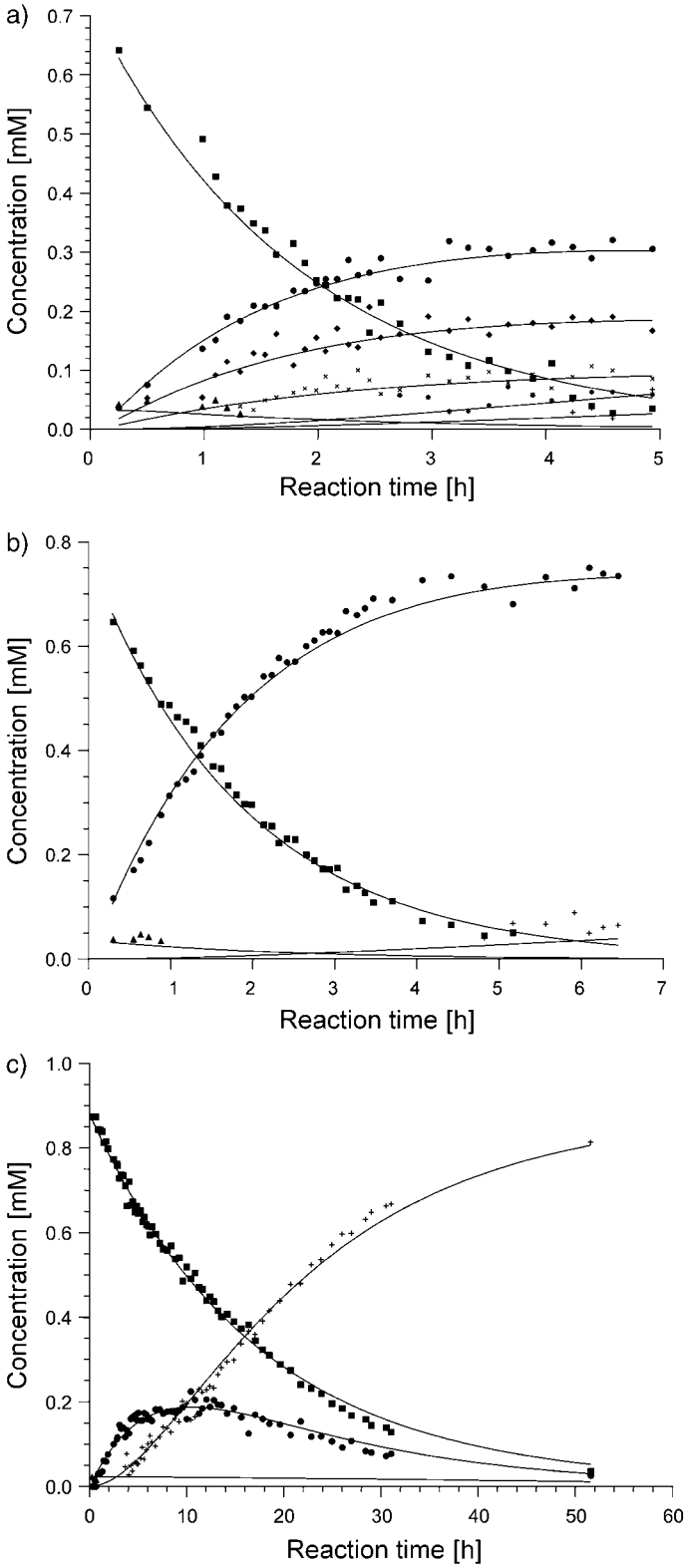

Figure 5. Experimental concentrations (NMR data) and theoretically fitted curves for the reaction between a) 0.72 mM *trans-EE* and 0.92 mM duplex **III** (pH 5.7, 20 mM $NaClO_4$, 20 mM phosphate buffer), b) 0.80 mM *trans-EE* and 1.6 mM duplex **IV** (pH 5.8, 100 mM $NaClO_4$), and c) 0.90 mM dichloro *cis*-DDP and 0.95 mM duplex **IV** (pH 5.7, 100 mM $NaClO_4$). All experiments were performed at 298 K. Symbols for a) and b): (■) dichloro *trans-EE*, (▲) monoaqua monochloro *trans-EE*, (●), (♦), and (×) G-N7/monochloro *trans-EE*, (+) G-N7/monoaqua *trans-EE*. Symbols for c): (■) dichloro *cis*-DDP, (▲) monoaqua monochloro *cis*-DDP, (●) G-N7/monochloro *cis*-DDP, (+) *cis*-DDP/[(G-N7)(G-N7)].

EE species (7.50/87.26 and 7.60/90.38 ppm, respectively). After 15 h, when almost all free *trans-EE* has disappeared, a second product starts to appear (8.13/94.31 ppm) and reaches about 10% of the total intensity after 21 h. The sample was left to stand for one week before a second 2D [^{1}H,^{15}N] HMQC NMR spectrum was recorded; this spectrum showed that the second product had now reached 30% of the total. This second product was assumed to be the aquated *trans-EE*/G-N7 adduct based on comparison with chemical shifts of the GMP/monoaqua *trans-EE* adduct.[17]

The same reaction was repeated twice at higher temperature (298 K), with a Pt/duplex ratio of 1:2 and a pH value of 5.8 (Figure 5b) and with a Pt/duplex ratio of 1:1 and a pH value of 6.7 (Figure 6), respectively. The proton assignments unambiguously determine the terminal G^1 residue to be the reaction site of *trans-EE* in duplex **IV**.

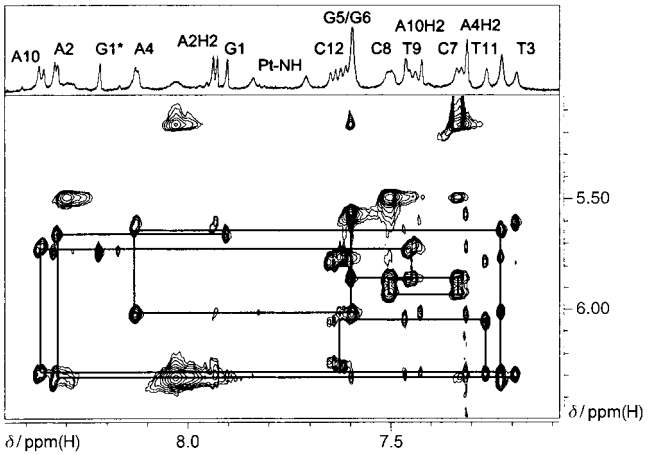

Figure 6. 2D [^{1}H,^{1}H] NOESY spectrum of 0.94 mM duplex **IV** and 1.0 mM dichloro *trans-EE* (100 mM $NaClO_4$, 5 mM phosphate buffer, pH 6.7) at 298 K. The peak labeled G1* is the platinated residue. All signals, except those from the central GC region and A^4-H2, are split into two peaks. In the peak group labeled A^{10}-H2 and T^9, the two smallest peaks are from T^9. The assignment was also carried on for the aromatic H2′/H2″ region, thereby confirming the assignment given here. In the aromatic H5′/H5″ region the terminal 5′ residue gives the most upfield-shifted signal which can help very much in the assignment of the G1 and G1* signals.

The rate constants for the reactions between *trans-EE* and **IV** (1:2 Pt/duplex ratio) performed at 285 K and 298 K are listed in Table 1.

Reaction of d(GATAGGCCTATC)$_2$ (IV) with *cis*-DDP: The reaction was carried out with equimolar amounts of reactants in 100 mM $NaClO_4$ and at pH 5.7 and 298 K. The first 2D [^{1}H,^{15}N] HMQC NMR spectrum, recorded after 15 min, shows three peaks at 4.04/−69.08, 4.06/−88.13, and 4.24/−67.34 ppm. The first one corresponds to dichloro *cis*-DDP and the other two to monoaqua monochloro *cis*-DDP. The spectrum recorded 50 min after the reaction was started exhibits two new signals, which represent the platinated product (NH_3 cross-peaks at 4.02/−69.97 ppm for *trans* Cl and 4.09/−65.33 ppm for *trans* N7). This product is assumed to be the monofunctional adduct of either G^5 or G^6. It was not possible from the 1D ^{1}H NMR spectra to unambiguously determine which of the two guanine residues was platinated first. In the imino region, the signal of G^5-N1 decreases and a new signal appears downfield of the imino signals of the three guanines. Previous studies have shown that the 5′-G of a GGCC sequence is more readily platinated than the 3′-G.[16] Therefore, the first product is most probably the monofunctional adduct at G^5. Shortly after the appearance of this first product, a second product appears (4.42/−69.34 and 4.29/−68.50 ppm) and, from the shift in the 2D [^{1}H,^{15}N] HMQC spectrum, this product is assigned as the G^5–Pt–G^6 chelate. No other products were detected within the following two days; thus, the terminal G residue appears to have a much lower affinity for *cis*-DDP than the central GG site. The presence of a G^5/G^6 cross-link was confirmed by NOESY spectra (one in H_2O and one in D_2O) which show two G^5/G^6-H8 signals shifted downfield by 0.68 ppm and 0.62 ppm, respectively. A corresponding downfield shift was not observed for the G^1-H8 signal. The formation of a A^4–Pt–G^5 chelate is less likely since no downfield-shifted A^4-H8 signal was observed. (For example, in an AG *cis*-DDP cross-linked nonanucleotide duplex the A-H8 resonance was found to be shifted 0.85 ppm downfield.[19]) Experimental concentrations (NMR spectroscopy data) and theoretically fitted curves for the reaction are reported in Figure 5c. The rate constants for G^5 platination and chelate formation are reported in Table 2.

Discussion

The differences in antitumor activity between *cis*- and *trans*-platinum(II) species have been related to three central factors: 1) the structural perturbation of DNA induced by platination, 2) the kinetics of adduct formation, and 3) the sequence selectivity of binding to DNA. We have already elucidated the kinetics of *trans-EE* binding to a mononucleotide (GMP)[17,20] and to a series of dinucleotides (rApG, dApG, and dGpA).[18] Therefore, in this work we wanted to investigate the interaction of *trans-EE* with single- and double-stranded oligonucleotides.

Reaction with single-stranded oligonucleotides: The platination sites in the two sequences investigated are clearly identified as being residues G^5 and G^5,G^6 for d(CCTCGCTCTC) (**V**) and d(CCTGGTCC) (**VI**), respectively. One may notice that G^5 and G^6 of **VI** have approximately equal affinity towards *trans-EE*. This is in agreement with our earlier data showing that sequence selectivity is absent in single-stranded metallation, but occurs in duplex DNA as a consequence of the variation in π-stacking interactions between base residues along the duplex.[16] The rate constants (Table 1) are comparable to those observed for adduct formation between *trans-EE* and dinucleotides.[18] No bifunctional adducts were observed within 24 h after mixing. In a control experiment, when **V** was treated with *cis*-DDP, the monofunctional G adduct formed initially slowly evolved into intrastrand G–Pt–C cross-links with neighboring cytosines. The rate constants for monofunctional and bifunctional adduct formation are listed in Table 2.

Bifunctional adducts with single-stranded oligonucleotides are formed not only by *cis*-DDP, as shown above, but also by *trans*-DDP. Therefore, the bulkiness of the carrier ligands must be responsible for the lack of formation of such cross-links in the case of *trans-EE*. Moreover, in a structural analysis of a *trans-EE* platinated duplex (formed by platination at G-N7 of **V** and subsequent hybridization with its complement 5′-d(GAGAGCGAGG)),[13] it was shown that the monofunctionally platinated duplex did not evolve to form an interstrand cross-link, but underwent a deplatination reaction over time (months). Thus, the intrastrand and interstrand DNA cross-links induced by *cis*-DDP and assumed to be important for its antitumor efficacy are not the critical lesions for *trans-EE*.

Reaction with double-stranded oligonucleotides lacking terminal G residues: Quite unexpectedly, the double-helical sequences d(TATGGCCATA)$_2$ (**I**) and d(TATGGTACCATA)$_2$ (**II**), with no terminal G residues, form only minor adducts with *trans-EE* (<5%) as determined by HPLC and 2D proton NMR spectroscopy. The amount of reaction products was not large enough to allow their characterization by 2D [^{1}H,^{1}H] NOESY spectra and thus it could not be determined if *trans-EE* platination follows the proposed rule for sequence-selective metallation.[16] In contrast, several platinated species were formed by using a large excess of *trans-EE* and prolonged heating (duplex **II**). The greater steric demand of imino ether ligands, as compared to NH_3, can account for the lack of affinity of *trans-EE* for G residues in the central parts of the duplexes, GGCC (**I**) and GGTA (**II**). This result is in line with the large conformational change induced by *trans-EE* platination of duplex **III**. (Such a monofunctional adduct was obtained by platination at G-N7 of the single-stranded 5′-d(CCTCG*CTCTC) (**V**) and subsequent hybridization with its complementary strand.[13]) Interestingly, the monofunctional platination by *trans-EE* was found to induce a bending of the helix axis towards the minor groove of approximately 40°, a bend comparable to that given by bifunctional adducts of *cis*- DDP which, however, is directed towards the major groove.

Reaction with double-stranded oligonucleotides containing terminal G residues: Duplexes **III** and **IV** contain both terminal and interior G residues. Both **III** and **IV** form adducts with *trans-EE* through the terminal G residues while the central G residues show no affinity. In the control experiment between **IV** and *cis*-DDP the central G residues were attacked by platinum to form a monofunctional adduct which was subsequently involved in forming an intrastrand G–Pt–G chelate. The terminal G residues, which were the only residues with affinity towards *trans-EE*, did not bind at all to *cis*-DDP (at least in a 1:1 *cis*-DDP/duplex ratio).

The rate constant for the formation of a monofunctional *trans-EE*/**III** adduct was found to be appreciably lower than the value obtained for monofunctional adduct formation between [Pt(dien)Cl]$^+$ and G residues of an analogous double-helical oligonucleotide.[16]

Conclusion

In a cell-free system (310 K, 10 mM $NaClO_4$), the monochloro mononitrato *trans-EE* complex has been found to interact with nondenatured calf thymus DNA (ctDNA) with $t_{1/2} = 294$ min as compared to 141 min for *trans*-DDP.[12,21] After approximately 48 h, the imino ether compound was bound quantitatively. Similar results were found by Coluccia et al. using a sample of ctDNA in 2 mM tris(hydroxymethyl)aminomethane (Tris)/HCl at pH 7.4.[22] The apparent discrepancy between these ctDNA results and the present study of double-stranded oligonucleotides may be rationalized by invoking a possible difference in the relative amount of unpaired nucleotides present in solution. The low amount of salt used in the ctDNA studies (10 mM $NaClO_4$ and 2 mM Tris/HCl, respectively) could have favored the presence of a large fraction of single-stranded DNA in the samples kept at 310 K. By contrast, in model systems of short oligonucleotides (like those used in the present investigation) it is much easier to control the equilibrium between single- and double-stranded species. The present results are also consistent with the hypothesis that *trans*-platinum imio ether complexes bind to DNA in a manner fundamentally different not only from that of *cis*-DDP but also from that of *trans*-DDP.[21] Characteristic features of *trans-EE* are a very large difference in reactivity towards single- and double-stranded oligonucleotides and the almost complete inability to form DNA cross-links. This leaves open the possibility that DNA–protein cross-links are responsible for the anticancer activity of *trans-EE*.[14] Moreover the sterically demanding imino ether ligands can also slow down the rate of hydrolysis and may also prevent (or retard) inactivation by sulphur-containing biomolecules. In conclusion, the role of carrier ligands in influencing the type and rate of formation of adducts with DNA and other relevant biomolecules is a field worthy of further investigation in the search for new anticancer agents.

Experimental Section

Materials: The ^{15}N-labeled *trans-EE* and ^{15}N-labeled *cis*-DDP complexes were prepared by the published procedures.[23] The DNA oligonucleotides were purchased from DNA Technology A/S (Aarhus, DK) and obtained as crude products from ethanol precipitation, except d(CCTGGTCC) (**VI**) which was obtained from Oswel DNA Service (Southampton, UK) as an HPLC-purified sample. The following chemicals were used for DNA purification and sample preparation: acetonitrile, triethylammonium acetate buffer (made from equimolar amounts of triethylamine and acetic acid), sodium hydrogen phosphate, NaCl, NaOH (all of them purchased from Baker), and sodium perchlorate (purchased from Merck).

Sample preparation: The purity of the oligonucleotides was first checked by HPLC (Waters 626 LC instrument with Millennium 32 software) on a MonoQ HR 10/10 (Pharmacia Biotech) column. If the samples were pure, the oligonucleotides were desalted on a Sephadex G-25 column (NAP-10, Pharmacia Biotech) with phosphate buffer (10 mM, pH 6.6) as the eluent. If the HPLC traces showed more than 5% of by-products, the oligonucleotides were purified on the MonoQ column and desalted on a LiChrospher 100 Rp-18 column (250×4 ID, 5 μm, Merck). Eluents used with the MonoQ column were A: 10 mM NaOH, 0.3 M NaCl, pH 12.5, and B: 10 mM NaOH, 1.0 M NaCl, pH 12.5. The linear gradients used for

the different oligonucleotides were as follows: duplex **I** (GGTA): 40→60% B in 30 min; duplex **II** (GGCC): 40→45% B in 30 min; single-stranded **III** (pyrimidine reach strand): 30→37% B in 30 min; single-stranded **III** (purine reach strand): 50→65% B in 30 min. The eluents used for desalting on the LiChrospher column were A: 5% acetonitrile, 15 mM triethylammonium acetate (TEAA), pH 7.2, and B: 70% acetonitrile, 15 mM TEAA, pH 7.2. A 30 min linear gradient from 0→15% B was applied for the desalting. TEAA and acetonitrile were removed by freeze-drying the sample twice, once at pH 12 and once at pH 3. This procedure was performed for all oligonucleotides except duplex **IV**, which was purified with dialysis at 5 °C in a 900-mL water bath containing 10 mM $NaClO_4$ and by using a Float-A-Lyzer (1 mL, 1000 Da molecular-weight cut off, Spectrum Laboratories, Inc., USA). The dialysis was performed over 4×3 h cycles (changing the reservoir each time). The purity was then checked by 1D ^{1}H NMR spectroscopy.

The kinetics were usually run at 298 K with samples containing 0.1 M $NaClO_4$ and 10–20 mM phosphate buffer. The concentrations of the oligomers were normally in the range 0.5–1 mM and the reactions were run at stoichiometric ratios except when stated otherwise. *trans-EE* was added to the DNA samples from a stock solution (superdistilled water saturated with *trans-EE* at ≈1.7 mM) and the ratio of Pt/DNA was determined by comparing the integral of the methyl group of *trans-EE* and the thymine methyl groups of the oligonucleotide in the 1D ^{1}H NMR spectrum. *cis*-DDP was added from a 2.42 mM solution prepared by dissolving (with sonication) *cis*-DDP (0.0070 g) in H_2O (9.5678 g). The reactions were carried out directly in the NMR spectroscopy tube (Wilmad 528 pp).

The reaction mixtures were separated on a MonoQ HR 10/10 column by using the same eluents as for the purification of the oligonucleotides. The reaction mixture of duplex **I** (GGTA) and *trans-EE* was separated by a linear gradient of 40→60% B over 30 min. Each of the collected fractions from the HPLC was then desalted on a Sephadex G-25 column (NAP-10, Pharmacia Biotech) with phosphate buffer (10 mM, pH 6.6) as the eluent.

NMR spectroscopy experiments: NMR experiments were performed on a Bruker DRX 600 or Varian Unity Inova 600 apparatus. Each instrument was fitted with a pulsed gradient module and a 5-mm inverse probehead. The Bruker instrument was used for the acquisition of 2D [^{1}H,^{15}N] HMQC, 2D [^{1}H,^{1}H] NOESY, and 1D ^{1}H NMR spectra. The dpfgsew5 pulse sequence was used for the suppression of water in 2D [^{1}H,^{1}H] NOESY and 1D ^{1}H spectra in H_2O.[24a,b] The 2D [^{1}H,^{15}N] HMQC NMR spectra were recorded in a phase-sensitive mode with the Echo/Antiecho-TPPI quadrature detection scheme. Pulsed field gradients were employed to select the proper coherence and the ^{15}N spins were decoupled during acquisition. No extra pulse sequence was needed for the suppression of water in 2D [^{1}H,^{15}N] HMQC spectra (pulse sequence of Palmer et al.)[25] in H_2O. The 2D [^{1}H,^{15}N] HMQC spectra were optimized for $^1J_{NH}$=72 Hz for *cis*-DDP and $^1J_{NH}$=78 Hz for *trans-EE*. The parameters for the 2D [^{1}H,^{15}N] HMQC experiments were as follows for *cis*-DDP: spectral width in *F*1 was 2006 Hz and in *F*2 was 4195 Hz, 2048 complex points in each FID in t_2 and 64 increments in t_1, 4–16 transients were averaged for each increment, and a relaxation delay of 2 s was used. 2D [^{1}H,^{15}N] HMQC parameters for *trans-EE*: spectral width in *F*1 was 1216 Hz and in F2 was 6010 Hz, 2048 complex points in each FID in t_2 and 32 increments in t_1, 8–16 transients were averaged for each increment, and a relaxation delay of 2 s was used. The Varian instrument was only used to record 1D ^{1}H and 2D [^{1}H,^{1}H] NOESY spectra of duplex **IV** (with the Watergate 3919 pulse sequence for water suppression).[26] The spectral width used for 1D ^{1}H and 2D [^{1}H,^{1}H] NOESY NMR data sets was 12019 Hz for all samples. The 2D [^{1}H,^{1}H] NOESY NMR spectra were recorded in a phase-sensitive mode by using the States-TPPI quadrature detection scheme.[27] A total of 2048 complex points in t_2 were collected for each of 512 t_1 increments, 24–48 transients were averaged for each increment, and a 1.7–2.0 s relaxation delay was applied. ^{1}H spectra were referenced to the HDO resonance set at 4.76 ppm or sodium 3-trimethylsilyl-2,2′,3,3′-tetradeuteropropionate (TSP) set to 0 ppm and ^{15}N spectra referenced to 1 M ^{15}N-enriched NH_4Cl in 1 M HCl solution set at 0 ppm. The 1D ^{1}H, 2D [^{1}H,^{1}H] NOESY, and 2D [^{1}H,^{15}N] HMQC NMR Bruker data were processed by using the program XWIN-NMR, version 2.6. The apodization function used in both dimensions for the 2D NMR data was a pure squared-cosine-bell. Window functions applied to the 1D ^{1}H FIDs were an exponential function with a line-broadening of 1–3 Hz or a gauss multiplication with a line-broadening of −1 Hz and gm 0.1. The t_1 FIDs in the 2D NMR data sets were linearly predicted to four times their original value. The Varian data was processed by using the program MestRe-C, version 3.4.0. (The same processing parameters as for the Bruker data were used.[28])

Data analysis: The rate constants for the reactions were determined by a nonlinear optimization procedure with the program SCIENTIST.[29] The data were fitted by using first- and second-order rate equations.

Acknowledgements

We thank the Norwegian Research Council (Contract 135055/432), the University of Bari, and the Italian M.I.U.R. (Cofin. N. 2001053898) for financial support. The University of Tromsø has to be acknowledged for the use of their Varian Unity Inova 600 instrument. We have also benefited from stimulating discussions with working group members of the COST Action D20.

[1] *Cisplatin-Chemistry and Biochemistry of a Leading Anticancer Drug* (Ed.: B. Lippert), Wiley-VCH, Weinheim, **1999**.
[2] A. M. J. Fichtinger-Schepman, A. T. van Oosterom, P. H. M. Lohman, F. Berends, *Cancer Res.* **1987**, *47*, 3000–3004.
[3] P. M. Takahara, C. A. Frederick, S. J. Lippard, *J. Am. Chem. Soc.* **1996**, *118*, 12309–12321.
[4] D. Z. Yang, S. S. G. E. van Boom, J. Reedijk, J. H. van Boom, A. H. J. Wang, *Biochemistry* **1995**, *34*, 12912–12920.
[5] A. Gelasco, S. J. Lippard, *Biochemistry* **1998**, *37*, 9230–9239.
[6] G. Natile, M. Coluccia, *Coord. Chem. Rev.* **2001**, *216–217*, 383–410.
[7] M. Coluccia, A. Nassi, F. Loseto, A. Boccarelli, M. A. Mariggiò, D. Giordano, F. P. Intini, P. Caputo, G. Natile, *J. Med. Chem.* **1993**, *36*, 510–512.
[8] N. Farrell in *Metal Ions in Biological Systems*, *Vol. 32* (Eds.: A. Siegel, H. Siegel), Marcel Dekker, New York, **1996**, pp. 603–639.
[9] L. R. Kelland, C. F. J. Barnard, I. G. Evans, B. A. Murrer, B. R. C. Theobald, S. B. Wyer, P. M. Goddard, M. Jones, M. Valenti, A. Bryant, P. M. Rogers, K. R. Harrap, *J. Med. Chem.* **1995**, *38*, 3016–3024.
[10] N. Farell, L. R. Kelland, J. D. Roberts, M. van Beusichen, *Cancer Res.* **1992**, *52*, 5065–5072.
[11] M. Coluccia, A. Boccarelli, M. A. Mariggiò, P. A. Caputo, F. P. Intini, G. Natile, *Chem. Biol. Interact.* **1995**, *98*, 251–266.
[12] R. Zaludova, A. Zakovska, J. Kasparkova, Z. Balcarova, O. Vrana, M. Coluccia, G. Natile, V. Brabec, *Mol. Pharmacol.* **1997**, *52*, 354–361.
[13] B. Andersen, N. Margiotta, M. Coluccia, G. Natile, E. Sletten, *Met. Based Drugs* **2000**, *7*, 23–32.
[14] O. Novakova, J. Kasparkova, J. Malina, G. Natile, V. Brabec, *Nucleic Acids Res.* **2003**, *31*, 6450–6460.
[15] a) M. Leng, D. Locker, M. J. Giraud-Panis, A. Schwartz, F. P. Intini, G. Natile, L. Pisano, A. Boccarelli, D. Giordano, M. Coluccia, *Mol. Pharmacol.* **2000**, *58*, 15–35; b) J. Kasparkova, V. Marini, Y. Najajreh, D. Gibson, V. Brabec, *Biochemistry* **2003**, *42*, 6321–6332.
[16] J. Vinje, J. A. Parkinson, P. J. Sadler, T. Brown, E. Sletten, *Chem. Eur. J.* **2003**, *9*, 1620–1630.
[17] Y. Liu, F. C. Intini, G. Natile, E. Sletten, *J. Chem. Soc. Dalton Trans.* **2002**, 3489–3495.
[18] Y. Liu, J. Vinje, C. Pacifico, G. Natile, E. Sletten, *J. Am. Chem. Soc.* **2002**, *124*, 12854–12862.
[19] M.-H. Fouchet, E. Guittet, J. A. H. Cognet, J. Kozelka, C. Gauthier, M. Le Bret, K. Zimmermann, J-C. Chottard, *J. Bioinorg. Chem.* **1997**, *2*, 83–92.
[20] Y. Liu, M. F. Sivo, G. Natile, E. Sletten, *Met. Based Drugs* **2000**, *7*, 169–176.
[21] V. Brabec, O. Vrana, O. Novakova, V. Kleinwachter, F. P. Intini, M. Coluccia, G. Natile, *Nucleic Acids Res.* **1996**, *24*, 336–341.

[22] M. Coluccia, A. Boccarelli, M. A. Mariggiò, N. Cardellicchio, P. Caputo, F. P. Intini, G. Natile, *Chem. Biol. Interact.* **1995**, *98*, 251–266.
[23] a) R. Cini, P. Caputo, F. P. Intini, G. Natile, *Inorg. Chem.* **1995**, *34*, 1130–1137; b) S. J. S. Kerrison, P. J. Sadler, *J. Chem. Soc. Chem. Commun.* **1977**, 861–864.
[24] a) A. M. Liu, X. Mao, C. Ye, H. Huang, J. K. Nicholson, J. C. Lindon, *J. Magn. Reson.* **1998**, *132*, 125–129; b) T.-L. Twang, A. J. Shaka, *J. Magn. Reson.* **1995**, *112*, 275–279.
[25] a) A. G. Palmer, J. Cavanagh, P. E. Wright, M. Rance, *J. Magn. Reson.* **1991**, *93*, 151–170; b) L. E. Kay, P. Keifer, T. Saarinen, *J. Am. Chem. Soc.* **1992**, *114*, 10663–10665.
[26] a) M. Piotto, V. Saudek, V. Sklenar, *J. Biomol. NMR* **1992**, *2*, 661–666; b) V. Sklenar, M. Piotto, R. Leppik, V. Saudek, *J. Magn. Reson. Ser. A* **1993**, *102*, 241–245.
[27] D. J. States, R. A. Haberkorn, D. J. Ruben, *J. Magn. Reson.* **1982**, *48*, 286–292.
[28] MestRe-C, version 3.4.0, http://www.mestrec.com.
[29] SCIENTIST, version 2.0, Micromath Scientific Software, Salt Lake City.

Received: February 5, 2004
Published online: June 3, 2004

